Nuclear Magnetic Resonance Studies Demonstrate Differences in the Interaction of Retinoic Acid with Two Highly Homologous Cellular Retinoic Acid Binding Proteins†

Andrew W. Norris,‡ Ding Rong,§ D. André d'Avignon,|| Michael Rosenberger,⊥ Kenzabu Tasaki,|| and Ellen Li*,‡,§,#

Department of Medicine, Department of Biochemistry and Molecular Biophysics, and Department of Chemistry|, Washington University, St. Louis, Missouri 63110, and Hoffmann-La Roche, Nutley, New Jersey 07110

Received June 14, 1995; Revised Manuscript Received October 4, 1995⊗

ABSTRACT: Cellular retinoic acid binding protein-I (CRABP-I) and cellular retinoic acid binding protein-II (CRABP-II) are highly homologous, 15 kDa proteins which bind *all-trans*-retinoic acid. In the adult, CRABP-II is expressed predominately in the epidermis, while CRABP-I is expressed in a variety of tissues. To obtain structural information which could aid the design of more selective ligands, isotope-directed NMR methods were employed to observe the CRABP-bound conformation of ^{13}C-labeled retinoic acid and to identify its contact points with neighboring amino acids. Analysis of HMQC, HMQC-TOCSY, and ^{13}C-TOCSY-REVINEPT on CRABP-bound (2,3,6,7,8,9,10,11,19-^{13}C)- and (1,4,5,8,9,16,17,18,19-^{13}C)-*all-trans*-retinoic acid allowed the unambiguous assignment of all labeled protons and their attached ^{13}C resonances. The volumes of 16 olefinic proton−methyl NOE cross-peaks measured from 30-ms ^{13}C-(ω_2)-filtered ^{1}H NOESY experiments were used to determine the conformations about the 6-, 8-, and 10-single bonds of the retinoic acid polyene chain. These spectra show qualitatively distinct NOE patterns for the two CRABPs. Measured cross-peak volumes for CRABP-II bound retinoic acid were well predicted by a single, static conformation having a 6-s torsion angle of −60° skewed from a *cis* conformation. In contrast, for CRABP-I no single, static conformation was able to match the pattern of cross-peaks, suggesting motion about the 6-s bond. The measured cross-peaks were best described by 8-s and 10-s torsion angles of 180° ± 30°, a *trans* configuration, for both proteins. The pattern of intermolecular NOESY cross-peaks between ^{13}C-labeled protons in the ring portion of retinoic acid and protein protons were different between CRABP-I and CRABP-II. These differences coincide well with nearby amino acid substitutions in the recently reported X-ray structures of crystalline CRABP-I and CRABP-II and may assist rational design of selective ligands.

Retinoic acid is a physiologically active metabolite of vitamin A. Retinoic acid, as well as a number of its synthetic analogs, have profound effects on growth and differentiation and are used for the treatment of severe dermatological diseases and certain malignancies (Hong & Itri, 1994; Peck & DiGiovanna, 1994). The use of these compounds is limited by their concomitant toxicity and teratogenic potential (Hong & Itri, 1994). The effects of retinoic acid are directly mediated through nuclear retinoic acid receptors (RARs[1] and RXRs), which are ligand dependent transcriptional activators belonging to the steroid/thyroid receptor family (Mangelsdorf et al., 1994; Petkovich, 1992). The level of retinoic acid available to the nuclear receptors is modulated by two small (15 kDa), cytoplasmic proteins which bind *all-trans*-retinoic acid with very high affinity: cellular retinoic acid binding protein-I (CRABP-I) and cellular retinoic acid binding protein-II (CRABP-II) (Ong & Chytil, 1978; Bailey & Siu, 1988; Norris et al., 1994).

The two CRABP isoforms are highly homologous; mouse CRABP-I and -II share 73% amino acid identity (Giguère et al., 1990). CRABP-I exhibits a higher binding affinity for *all-trans*-retinoic acid than does CRABP-II (Bailey & Siu, 1988; Fiorella et al., 1993; Norris et al., 1994). The two isoforms have unique patterns of distribution. In adults CRABP-I is expressed in many tissues including lung, brain, and epidermis, while CRABP-II is highly expressed solely in the epidermis (Ong & Chytil, 1978; Giguère et al., 1990; Siegenthaler et al., 1992). Both CRABP isoforms are expressed during fetal development, with CRABP-II expressed in less quantity than CRABP-I but having a wider tissue distribution (Ruberte et al., 1992).

The CRABPs appear to limit the amount of *all-trans*-retinoic acid available to the RARs by sequestering retinoic acid and/or by promoting retinoic acid metabolism (Fiorella

† This work was supported by grants from the National Institutes of Health (DK-40172, DK-49684, DK-49694, and DK-02072).

* Address correspondence to this author at Department of Medicine, Washington University School of Medicine, Campus Box 8051, 660 South Euclid Ave., St. Louis, MO 63110. Telephone: (314) 362-1070. Fax: (314) 362-9230.

‡ Department of Biochemistry and Molecular Biophysics, Washington University.

§ Department of Medicine, Washington University.

|| Department of Chemistry, Washington University.

⊥ Hoffmann-La Roche.

Burroughs Wellcome Scholar in Toxicology.

⊗ Abstract published in *Advance ACS Abstracts,* November 1, 1995.

[1] Abbreviations: CRABP-I, mouse cellular retinoic acid binding protein-I; CRABP-II, mouse cellular retinoic acid binding protein-II; RAR, retinoic acid receptor; RXR, retinoid X receptor; iLBP, intracellular lipid binding protein; HMQC, heteronuclear multiple-quantum coherence; NOESY, nuclear Overhauser effect spectroscopy; TOCSY, total correlation spectroscopy; REVINEPT, reverse insensitive nucleus enhancement by polarization transfer; GARP, globally optimized alternating-phase rectangular pulses; NOE, nuclear Overhauser effect; TPPI, time-proportional phase incrementation; rms, relative root mean square error; CRBP, cellular retinol binding protein.

0006-2960/95/0434-15564$09.00/0 © 1995 American Chemical Society

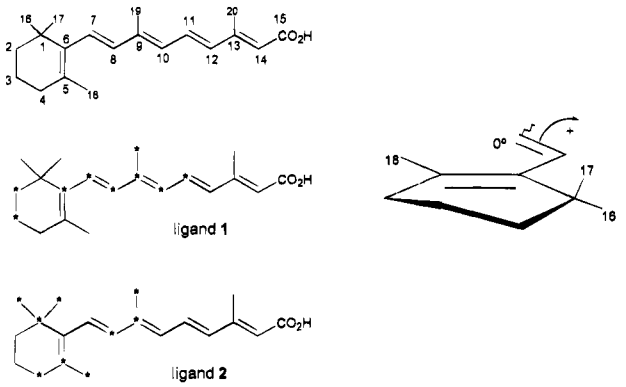

FIGURE 1: Established numbering convention for retinoic acid along with the ^{13}C-labeling schemes of ligand **1** and **2**. The half-chair conformation used as the starting conformation for the modeling of retinoic acid is shown as well as the convention chosen to number methyl groups 16 and 17. The 6-s torsion angle is defined by C5−C6−C7−C8, as shown.

& Napoli, 1991; Boylan & Gudas, 1991). Synthetic compounds which bind to the CRABPs but not to the nuclear receptors could modulate nuclear retinoid signaling by displacement of endogenous retinoic acid from the cytoplasmic to nuclear compartment. The development of more selective ligands for one of the two CRABPs may help delineate the physiological roles of each of the isoforms as well as provide new therapeutic agents which exhibit increased biological selectivity.

An understanding of the factors determining molecular recognition by the CRABPs is therefore important. On the basis of amino acid sequence and crystal structure, the CRABPs are members of the intracellular lipid binding protein (iLBP) family (Banaszak et al., 1994; Kleywegt et al., 1994). The recently reported crystal structures of bovine/murine CRABP-I and human CRABP-II complexed with *all-trans*-retinoic acid, at resolutions of 2.9 and 1.8 Å, respectively, are similar to structures of other members of the iLBP family, sharing the motif of two orthogonal β-sheets formed by 10 antiparallel β-strands (Kleywegt et al., 1994). As with other iLBPs, the ligand-binding cavity of the CRABPs is located within the two β-sheets. This binding cavity in the CRABPs differs significantly from the binding cavity of the cellular retinol binding proteins (CRBPs, which bind *all-trans*-retinol but not *all-trans*-retinoic acid). However, at this level of resolution few differences in ligand conformation and ligand−protein contact points were detected in comparing the crystal structures of CRABP-I and -II.

The use of NMR to study the three-dimensional structure of drug/receptor complexes has been facilitated by methods to selectively detect proton signals of isotopically labeled ligands bound to unlabeled receptors (Fesik, 1993). Isotope-edited NOE experiments provide information on the bound conformation of the ligands as well as ligand−protein close contacts. This information may aid in the design of more selective ligands. We report here the results of comparative isotope-edited NMR studies of ^{13}C-labeled *all-trans*-retinoic acid when complexed with CRABP-I and CRABP-II.

MATERIALS AND METHODS

NMR Sample Preparation. (2,3,6,7,8,9,10,11,19-^{13}C)-*all-trans*-Retinoic acid (ligand **1**) (see Figure 1) and (1,4,5,8,9,16,17,18,19-^{13}C)-13-*cis*-retinoic acid were kindly provided by Hoffmann-La Roche. The *all-trans* isomer (ligand **2**) of (1,4,5,8,9,16,17,18,19-^{13}C)-13-*cis*-retinoic acid was prepared by isomerizing the 13-*cis* bond in the presence of iodine (Kaegi & DeGraw, 1981). All procedures involving retinoic acid were performed in dim or red light. Recombinant mouse CRABP-I and CRABP-II were expressed and purified to homogeneity from *Escherichia coli* as described (Norris et al., 1994).

The samples used in the NMR studies contained 1.5 mM CRABP-I or CRABP-II complexed with ligand **1** or ligand **2** in 0.6 mL of 10 mM KPO_4, pH 7.4,[2] 0.05% NaN_3, and 99.8% D_2O. The samples were prepared by the addition of equimolar amounts of ^{13}C-labeled retinoic acid dissolved in microliter volumes of dimethyl sulfoxide-d_6 to a 0.1−0.2 mM solution of CRABP-I or CRABP-II. Both CRABPs bind *all-trans*-retinoic acid with an affinity strong enough to ensure essentially complete binding at these concentrations: $K_d' \leq 0.4$ nM and $K_d' = 2$ nM for CRABP-I and -II, respectively (Norris et al., 1994). The samples were then concentrated by ultrafiltration, followed by repeated exchanges with the D_2O buffer. Deuterium oxide was purchase from Sigma (St. Louis, MO) and dimethyl sulfoxide-d_6 from Cambridge Isotope Laboratories (Woburn, MA).

NMR Measurements. NMR spectra were recorded at 25 °C on Varian Unity and Unity Plus spectrometers operating at proton frequencies near 500 and 600 MHz. Heteronuclear decoupling was accomplished using GARP (Shaka et al., 1985). The residual water signal was suppressed using low-power preirradiation. All spectra were recorded and processed in the hypercomplex mode (States et al., 1982), except where noted. External TSP in buffer solution was used to reference proton and carbon chemical shifts. NMR data were processed and analyzed, including measurement of cross-peak volumes from 2-D NOESY spectra, using Varian VNMR software on SunSparc workstations.

Two-dimensional [$^1H-^{13}C$]HMQC, HMQC-TOCSY, and ^{13}C-TOCSY-REVINEPT were collected essentially as described previously (Gronenborn et al., 1989; Fesik et al., 1990a). The HMQC-TOCSY and ^{13}C-TOCSY-REVINEPT employed MLEV-17 spin lock (Bax & Davis, 1985) times of 10 and 12 ms, respectively. $^{13}C(\omega_2)$-filtered 2-D [^1H,^1H] NOESY spectra were acquired using the pulse sequence: $90°(^1H)-t_1-90°(^1H)-\tau_{mix}-90°(^1H)-1/2J_{C\text{-}H}-180°(^1H),90°-(^{13}C)\pm90°(^{13}C)-1/2J_{C\text{-}H}-$acquire($t_2$) (Fesik et al., 1990b). ^{13}C-decoupling was applied during t_1 and t_2. $J_{C\text{-}H}$ was set to 170 Hz. The recycling delay was 2.2 s. Two-dimensional, $^{13}C(\omega_1,\omega_2)$ double half-filter [^1H,^1H]NOESY spectra used a described pulse sequence (Wider et al., 1990), substituting ^{13}C-decoupling for the ^{13}C-decoupling pulse during t_1 and using delays of $1/2J_{C\text{-}H}$ for the filters. The phase cycle was altered so that the appropriate carbon and receiver phases to achieve the $^{13}C(\omega_1,\omega_2)$ selection were cycled every four scans. The spectra were recorded using TPPI (Marion & Wüthrich, 1983) in the t_1 dimension.

RESULTS

Assignments. Identification of protons directly bonded to the ^{13}C-labeled nuclei of ligands **1** and **2** complexed with CRABP-I and CRABP-II was made from analysis of $^1H-^{13}C$ correlation experiments. In the HMQC spectra shown in Figures 2 and 3, the olefinic, methylene, and methyl protons were readily identified from chemical shifts and

[2] pH readings were not corrected for isotope effects.

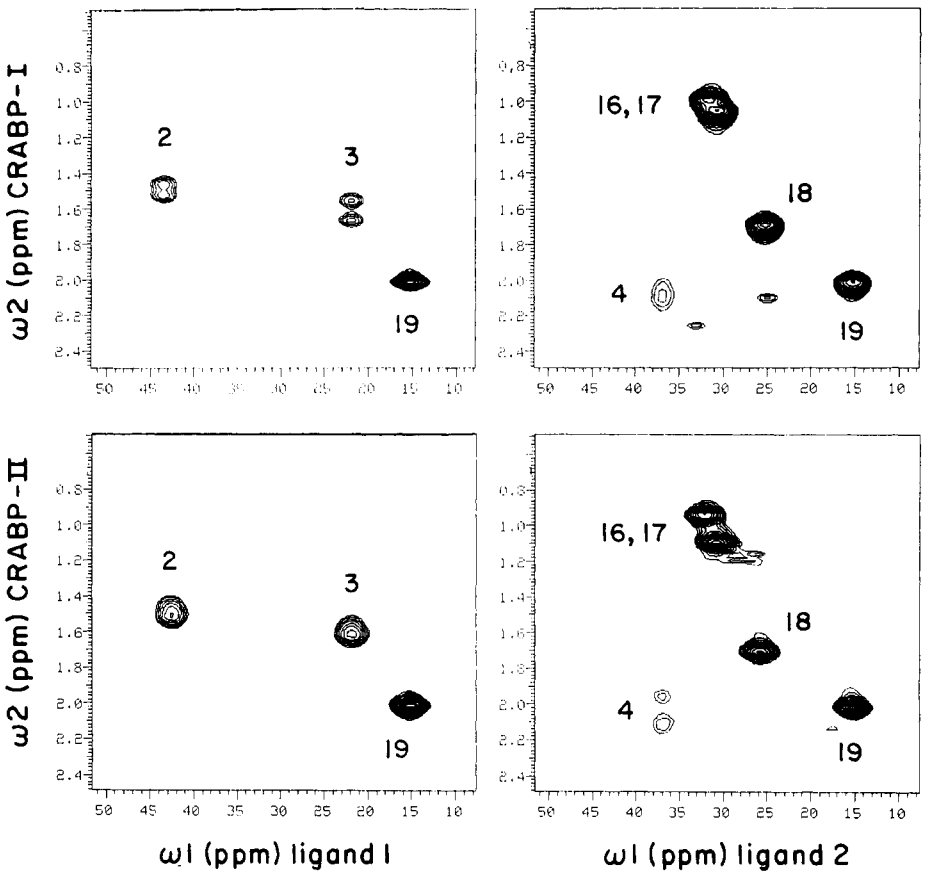

FIGURE 2: Aliphatic regions of HMQC spectra acquired on ligand **1** (left panels) and ligand **2** (right panels) complexed with CRABP-I (top panels) and CRABP-II (bottom panels). The HMQC spectra are the result of 109−400 total increments in t_1. Between 16 and 64 transients were collected per increment, at a proton frequency of ca. 600 MHz. ^{1}H 90°-pulse times were 9−13 μs; ^{13}C 90°-pulse times, 14−20 μs. Total acquisition times were 2.3−8.4 μs in t_1 and 0.163 s in t_2. To aid comparison, the HMQC spectra were treated with equivalent Gaussian functions.

signal intensities. The resonances corresponding to CH(8) and CH_3(19) were assigned by comparison of the HMQC spectra of ligands **1** and **2**, as these are the only ^{13}C-labeled protons common to both compounds. The CH_2(4) resonance was easily assigned, as it is the only labeled methylene in ligand **2**. The vicinal methyl resonances, CH_3(16) and CH_3(17), were distinguished from the CH_3(18) resonance by identification of the carbon scalar coupling between CH_3(16) and CH_3(17) through analysis of ^{13}C-TOCSY-RE-VINEPT spectra collected on CRABP-bound ligand **2** (data not shown). Specific assignment of these two methyl groups to the C16 or C17 position cannot be made on the basis of through-bond connectivities alone. The remaining methylene protons, CH_2(2) and CH_2(3), and olefinic protons, CH(7), CH(10), and CH(11), were assigned by analysis of HMQC-TOCSY spectra which revealed the following scalar couplings: CH_2(2)−CH_2(3), CH_2(3)−CH_2(4), CH(7)−CH(8), CH(10)−CH(11), and CH(11)−CH(12) (data not shown). The CH(11)−CH(12) coupling was not observed in CRABP-I, probably because of spectral overlap. In this case, CH-(11) was distinguished from CH(10) by observation of a strong NOE (see below) from CH_3(19), knowing that CH-(10), unlike CH(11), cannot closely approach CH(19) due to the 9−10 double bond.

The ^{13}C chemical shifts of retinoic acid bound to the two CRABPs are similar, and vary up to 2.2 ppm compared to those of free *all-trans*-retinoic acid (Waterhous & Muccio, 1990), with the exception of C11 which is shifted upfield ca. 5 ppm (see Supporting Information, Table 1S). The observed differences in chemical shift may arise from interaction with the surrounding protein and/or from conformational changes upon binding (Rowan & Sykes, 1974; Harbison et al., 1985). Disentanglement of these two effects is difficult. The conformational dependence of retinoid chemical shifts has been well studied. Isomerization about the 9−10 double bond to *cis* causes large (~8 ppm) shifts of C8 upfield and C19 downfield (Rowan & Sykes, 1974; Becker et al., 1974). In a separate effect, rotation of the 6-s single bond to a *trans* conformation causes an upfield shift of C8 of similar magnitude (Harbison et al., 1985). These large shifts are not observed in CRABP bound retinoic acid, arguing against these specific conformational changes. The vicinal ring methyls, CH_3(16) and CH_3(17), have nonidentical ^{13}C and ^{1}H chemical shifts when complexed with CRABP. This is in contrast to free retinoic acid, in which the chemical shifts of CH_3(16) and CH_3(17) are identical, most likely due to rapid reorientation of the 6-s bond and interconversion of the two half-chair ring conformers (Rowan & Sykes, 1974). (Figure 1 shows one of the two ring conformers.) It is thus likely that in the bound state at least one of these conformational freedoms has been lost or is in slow exchange, causing CH_3(16) and CH_3(17) to lose their chemical equivalence.

The ^{1}H chemical shifts of retinoic acid show very similar changes, up to 0.5 ppm, upon binding to the two CRABPs (Table 1S). Comparison of the HMQC spectra of CRABP bound retinoic acid reveals differences in the methylene proton resonances (Figure 2). Methylene groups CH_2(2) and CH_2(3) are each split into two resonances in CRABP-I bound retinoic acid, but not in CRABP-II bound retinoic acid.

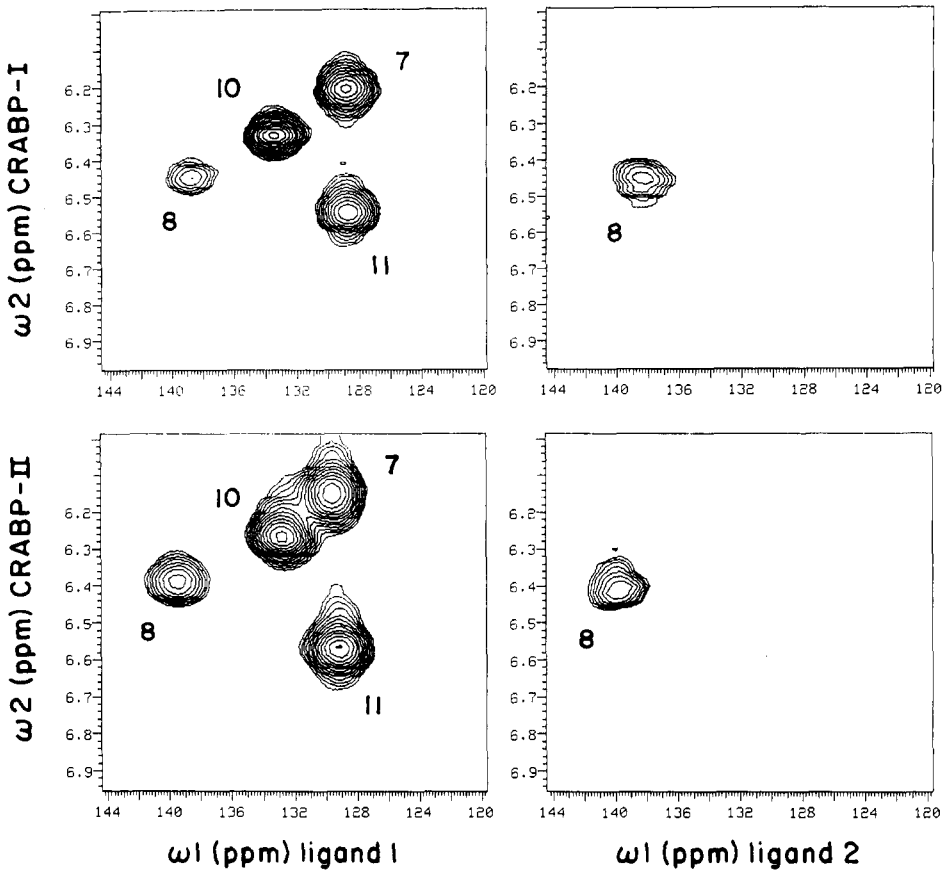

FIGURE 3: Olefinic regions of HMQC spectra acquired on ligand **1** (left panels) and ligand **2** (right panels) complexed with CRABP-I (top panels) and CRABP-II (bottom panels). These are from the same HMQC spectra as shown in Figure 2.

Methylene $CH_2(4)$ is split into two resonances in both CRABP−retinoic acid complexes. These methylene resonances are not split in free retinoic acid (Waterhous & Muccio, 1990). Constraint of the β-ionone ring to one of the two half-chair conformations, when bound, could result in methylene resonances split in the ^1H dimension, as seen in CRABP-bound retinoic acid. Alternative explanations for the observed methylene resonance splittings in the proton dimension, such as two slowly interconverting binding states, are also possible.

Conformational Analysis of CRABP Bound Retinoic Acid. The conformational flexibility of retinoic acid is limited by its double bonds and ring structure. However, conformational analysis of retinoids has shown conformational freedom about the single bonds of the polyene chain, especially the 6-s bond (Rowan et al., 1974; Honig et al., 1971; Stam & MacGillavry, 1963; Stam, 1972). NMR studies of free retinoids have used long-range coupling constants, spin−lattice relaxation times, chemical shifts, and steady-state nuclear Overhauser enhancements to define the torsion angles of the polyene chain single bonds (Honig et al., 1971; Rowan et al., 1974). Unfortunately, the coupling constants are too small (<12 Hz) to be measured in the CRABP bound state due to shortened T_2's (~10 ms), and the spin−lattice relaxation times and chemical shifts may be perturbed by the surrounding protein. These limitations have dictated our use of isotope-edited 2D-NOESY studies for conformational analysis of protein bound retinoic acid. To assess the effects of spin diffusion, NOE build-up curves were measured for selected cross-peaks observed in isotope-edited 2D-NOESY spectra of the CRABP-II−ligand **2** complex, at mixing times of 30, 50, 70, and 100 ms (see Figure 4). To minimize spin diffusion effects, subsequent NOESY experiments used the shortest mixing time amenable to evaluation of cross-peak volumes, 30 ms.

The isotope-edited 2-D NOESY spectra of ligand **1** complexed with CRABP-I and CRABP-II, and ligand **2** complexed with CRABP-I and CRABP-II, are shown in Figures 5 and 6, respectively. In the ω_2 dimension, only those protons attached to ^{13}C-labeled nuclei are detected. In the ω_1 dimension, NOE cross-peaks between "labeled" protons and other nearby protons are observed. The cross-peak assignments were based on the resonance assignments described above. To rule out the possibility of coincidental intermolecular cross-peaks, the identity of the following olefinic(ω_1)−methyl(ω_2) cross-peaks were confirmed by ^{13}C-(ω_1,ω_2) double half-filter [^1H,^1H]NOESY experiments which select only NOE cross-peaks where both involved protons are "labeled": CH(7)−CH_3(19), CH(11)−CH_3(19), and CH(8)−CH_3(18).

As shown in Figures 5 and 6, intense NOEs were observed between CH(7) and CH_3(19) and between CH(11) and CH_3(19). These NOEs are consistent with an 8-s *trans* and 10-s *trans* conformation of the polyene chain for retinoic acid in the CRABP bound state. NOEs between the following olefinic-proton/methyl pairs, CH(7)−CH_3(16), CH(7)−CH_3(17), CH(7)−CH_3(18), CH(8)−CH_3(16), CH(8)−CH_3(17), and CH(8)−CH_3(18), provide information about the orientation of the 6-s bond. An intense NOE cross-peak between CH(8) and CH_3(18) as well as an NOE cross-peak between CH(7) and CH_3(16/17) are present in the isotope-edited NOESY spectrum of the CRABP-II ligand **2** complex. No NOE cross-peak was observed between CH(7) and CH_3(18). These results are most consistent with a 6-s *cis* conformation.

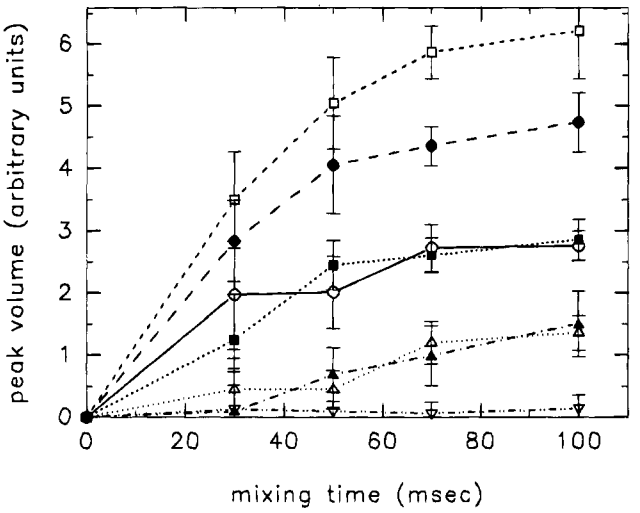

FIGURE 4: Build-up curve of selected NOE cross-peaks. $^{13}C(\omega_2)$-filtered ^1H NOESY spectra were acquired sequentially on ligand **2** bound to CRABP-II at mixing times of 100, 70 , 50 and 30 ms. The sample and spectrometer were not disturbed between runs. A total of 160 increments were acquired at each mixing time, collecting 192 transients per increment, at a proton frequency of ca. 500 MHz. The ^1H 90°-pulse time was 9.5 μs; the ^{13}C 90°-pulse time, 14 μs. Total acquisition times were 14.9 μs and 0.19 s in t_1 and t_2, respectively. The data were zero-filled to 1024 points in t_1 and 4096 points in t_2 and treated with equivalent Gaussian weighting functions. Uncertainties were estimated from the standard error of multiple (≥3) volume measurements plus the standard error of background. Cross-peaks ($\omega_1-\omega_2$) are as follows: 11−19 (□), 7−19 (●), protein (4.0 ppm)−19 (○), 8−18 (■), 7−16,17 (1.04 ppm) (△), 7−18 (▲), 8−16,17 (1.04 ppm) (▽).

In contrast, a relatively intense NOE cross-peak between CH-(7) and CH_3(18), a less intense NOE cross-peak between CH(8) and CH(18), and a weak NOE cross-peak between CH(8) and CH_3(16/17) are present in the isotope-edited NOESY spectrum of the CRABP-I ligand **2** complex. These results indicate that there are differences in the 6-s-torsion angle of retinoic acid when complexed with CRABP-I and with CRABP-II.

Conformational Modeling of CRABP-Bound Retinoic Acid. In order to obtain a more quantitative measurement of the polyene chain torsional angles, the relative volumes of the sixteen possible olefinic(ω_1)-methyl proton(ω_2) NOE cross-peaks observed in the isotope-edited NOESY spectra of CRABP-bound ligand **2** (see the boxed areas of Figure 6) were analyzed by systematic search as described below. To ascertain the possible perturbing effects of relaxation on these studies, T_1 values were measured by inversion recovery with an X-filtered read pulse. The T_1's for the involved resonances are much longer than the mixing time of 30 ms, ranging from 340 to 790 ms, and thus are expected to have little perturbation on the observed NOESY cross-peaks.

all-trans-Retinoic acid was constructed with standard geometries and bond lengths using Sybyl (Tripos, St. Louis, MO). The β-ionone ring was built in the half-chair conformation found in the crystal structures of the holo-CRABPs (Kleywegt et al., 1994), as shown in Figure 1. The other half-chair conformation is simply related by reflection (σ) of ring atoms across the plane described by C1, C6, C5, and C4. Sybyl was used to perform systematic searches, without minimization, over the rotatable single bonds C6−C7, C8−C9, and C10−C11 and to measure the desired interatomic distances and angles for all of the generated conformations. Searching the alternate ring conformer is not necessary, since it is equivalent to reversing the sign of the searched torsion angles (i.e., applying the σ operation to torsion angle rotation.) Relative volumes of olefinic−methyl proton NOEs for each conformation were calculated on the basis of the r^{-6} dependence of dipole−dipole interactions and by modeling each conformation as a single, static structure undergoing isotropic tumbling, with the exception of the methyl groups. The following four methyl group motional models were used: (i) three-jump site model undergoing fast rotation ($\tau_i < \tau_c$), where τ_i is the methyl group's rotational correlation time and τ_c is the correlation time of the overall tumbling of the complex (Morikis et al., 1993), (ii) three-jump site model undergoing slow rotation ($\tau_c < \tau_i$) (Morikis et al., 1993), (iii) full, rapid rotational model ($\tau_i < \tau_c$) (Pegg et al., 1980), and (iv) use of the centroid of the methyl protons (Honig et al., 1971). For each conformation generated by the systematic search, theoretical, relative NOE cross-peak volumes were calculated for the 16 olefinic-methyl pairs using each of these methyl models.

To evaluate which conformations best fit the experimental NOESY cross-peak volumes, the relative root-mean-square errors (rms) between modeled and experimental volumes

$$\text{rms} = \sqrt{\sum_{ik}(V_{ik}^{\text{exp}} - sV_{ik}^{\text{model}})^2}$$

were calculated for each conformation (Morikis et al., 1993) for methyls i and olefinic protons k. The scaling factor of the fit, s, was optimized for each conformation so as to minimize rms (Morikis et al., 1993). The fitting results from a systematic search performed by varying the 6-s, 8-s, and 10-s torsion angles at 15° intervals are shown in Figure 7. For both CRABPs, the best fitting model conformations have an 8-s and 10-s torsion angle of 180 ± 30°, i.e., a *trans* conformation. The best fitting 6-s torsion angle for retinoic acid complexed with CRABP-I is −75° (i.e., 285°), while the best fitting 6-s torsion angle for the CRABP-II complex is −60°. These are both skewed 6-s *cis* conformations, with a larger skew for CRABP-I. Note that for CRABP-II, the negative skew (−60°) yields a much better fit than the positive skew (+60°), but for CRABP-I the difference between a negative and positive skew is minimal.

Systematic search model conformations were evaluated for each of the two possible assignments of the vicinal methyl groups 16 and 17 (see Supporting Information, Table 2S). To avoid missing better-fitting conformations which may fall between search angles, these searches were performed on a finer grid: 3° for 6-s and 10° for 8-s and 10-s. For both CRABPs, assignment of the vicinal methyl peak at lower chemical shift to 16 yielded better fits, although the differential between assignments for CRABP-I is very small. Thus, only CRABP-II has been given this assignment (Table 1S). To ascertain the potential effects of methyl group motion on these results, fittings were performed for NOEs calculated using each of the four methyl group models. In every case the assignment of the vicinal methyl peak at lower chemical shift to 16 yielded the better fit. In addition, negative skews for 6-s always yielded better fits. The best fitting 8-s and 10-s torsion angles were 180 ± 30° for both CRABPs. The best fitting 6-s torsion angles calculated using each of the four methyl group models varied by no more than 6° for CRABP-I and 3° for CRABP-II, suggesting that

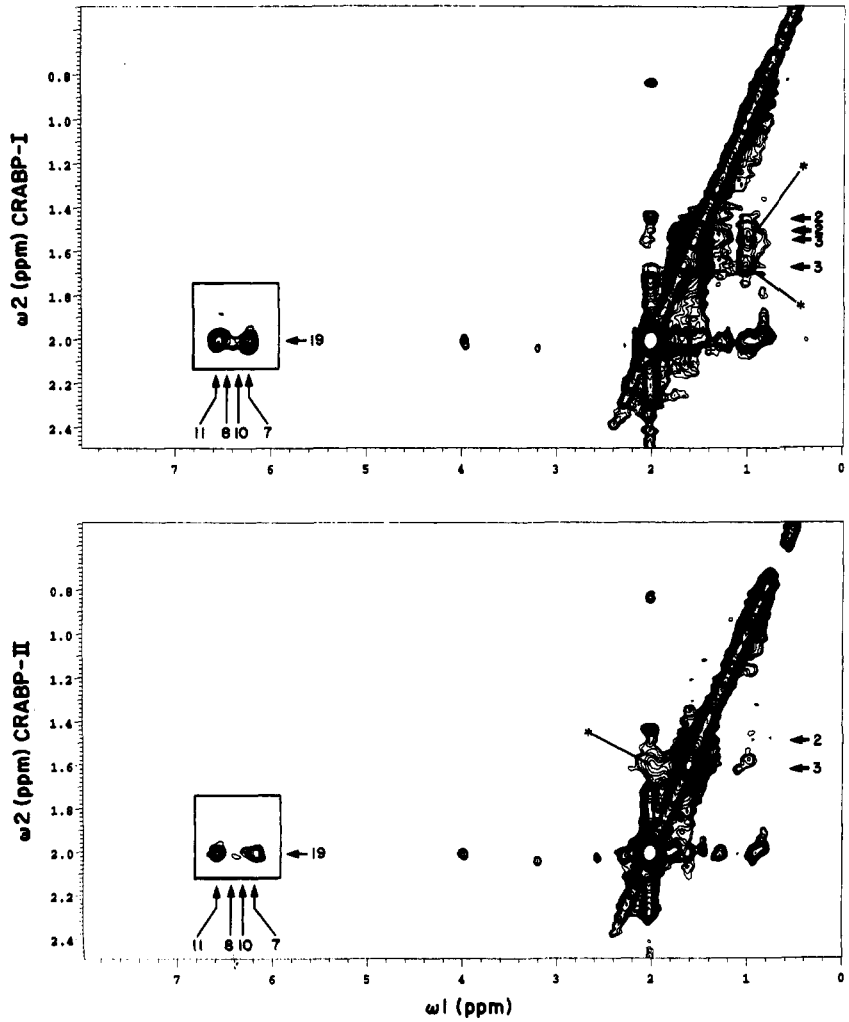

FIGURE 5: $^{13}C(\omega_2)$-filtered 2-D [^{1}H,^{1}H]NOESY acquired on ligand **1** bound to CRABP-I (top panel) and CRABP-II (bottom panel), using a mixing time of 30 ms. The spectrometer proton frequency was ca. 500 MHz. The ^{1}H 90°-pulse time was 9.5 μs; the ^{13}C 90°-pulse time, 15.5 μs. Total acquisition times were 19 or 22 μs in t_1 and 0.19 s in t_2. A total of 208 or 238 increments were collected using 192 or 144 transients per increment and processed as described in the legend to Figure 4. The scale of these spectra have been matched by normalizing the maximum intensity of methyl 19's diagonal peak to the same height for both CRABPs. The boxed areas contain intra-retinoic acid olefinic(ω_1)−methyl (ω_2) cross-peaks. The stars point to nonconserved intermolecular cross-peaks.

our results are relatively independent of the methyl model adopted.

These skewed *cis* conformations fall within energetically favorable portions of the potential for the 6-s bond. Semi-empirical molecular orbital calculations found a narrow minima at 180° (i.e., *trans*) and a broad minima from 40° to 120° (i.e., skewed *cis*) (Honig et al., 1971). Our measured 6-s conformations correspond, as well, to the 6-s conformation measured by NMR for retinal in solution of 30−70° (Honig et al., 1971). These skewed *cis* conformations are in good agreement with our measured C8 chemical shifts of ca. 136−137 ppm. Distorted 6-s *cis* retinoic acid and derivatives have been found to consistently have C8 chemical shifts of 138−140 ppm, while 6-s *trans*-retinoic acid and derivatives have C8 chemical shifts of ca. 130−133 ppm (Harbison et al., 1985).

Possible Motion of CRABP-I Bound Retinoic Acid. Table 1 compares the experimentally measured NOESY cross-peak volumes with the best-fit modeled volumes and shows good agreement for CRABP-II. Three moderate discrepancies are present in that the experimentally measured volumes for 7−18, 7−17, and 7−16 are not as large as predicted. These are modeled to be moderately small peaks and may thus be difficult to observe, especially at short mixing times. Other sources of potential error include spin diffusion, potential motion, variations from ideal geometry, and errors in volume measurement. The agreement between experimental and modeled cross-peak volumes is much poorer in CRABP-I, with a notable discrepancy for 7−18, in that the model is unable to account for the large measured peak for this interaction. There are smaller discrepancies for 7−17, 7−16, and 8−17. Thus, for CRABP-I, the best fitting model conformation has poorly matched the pattern of NOEs which define the 6-s torsion angle.

To address the ability of the modeled conformations to predict the pattern of NOEs which directly define the 6-s torsion angle, additional fits were performed using a truncated data set consisting only of these cross-peaks: 7−16, 7−17, 7−18, 8−16, 8−17, and 8−18. Theoretical NOEs calculated from conformations generated by systematic search about the 6-s bond at 1° intervals were fit to the truncated datasets. For CRABP-II the best fit 6-s conformations were skewed ±36−47° from *cis*, having excellent rms's as low as 5.4 out of 76.4 maximally possible. The best fits for CRABP-I were very poor, having 6-s conformations skewed −70 to −82° from *cis*, and lowest rms's of 35.8 out of 59.4 maximally possible. These results agree with the conclusions drawn from Table 1 that the model conforma-

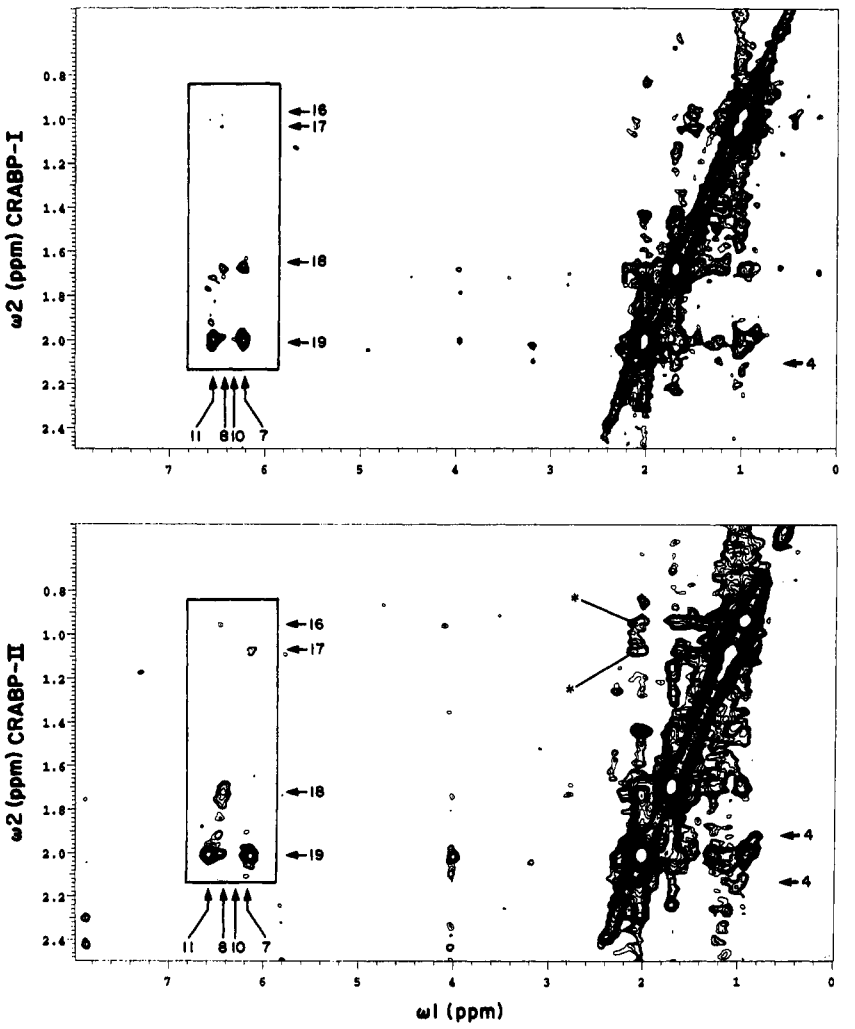

FIGURE 6: $^{13}C(\omega_2)$-filtered 2-D [^{1}H,^{1}H]NOESY acquired on ligand **2** bound to CRABP-I (top panel) and CRABP-II (bottom panel) using a mixing time of 30 ms. The spectrometer proton frequency was ca. 500 MHz. The ^{1}H 90°-pulse time was 9.5 μs; the ^{13}C 90°-pulse time, 14 μs. Total acquisition times were 34 or 19 μs in t_1 and 0.19 s in t_2. A total of 366 or 200 increments were collected using 224 or 256 transients per increment and processed as described in Figure 4. The boxed areas contains the intra-retinoic acid olefinic(ω_1)−methyl (ω_2) cross-peaks which were used in the conformational analysis. The stars point to nonconserved intermolecular cross-peaks.

tions are unable to predict the pattern of NOEs in CRABP-I which define the 6-s torsion angle.

To aid understanding of factors which may contribute to this discrepancy in CRABP-I, modeled cross-peak volumes for these interactions are plotted versus the 6-s torsion angle in Figure 8. The horizontal line in this plot represents the cross-peak volume expected for the closest approach of 7 and 19. Because 7−19 is essentially the largest olefinic−methyl cross-peak measured in our spectra, all other cross-peaks are smaller and should fall below this line. First note that −60° yields a good fit for CRABP-II, providing a strong 8−18 cross-peak, a moderately small 7−17 cross-peak, and smaller cross-peaks at other positions. With regard to CRABP-I, note that for no single 6-s angle can there be a simultaneous moderate sized cross-peak for both 8−18 and 7−18. This is the reason that the best fit CRABP-I conformation failed to predict the large cross-peak observed for 7−18. One explanation for the appearance of both of these cross-peaks in CRABP-I is motion about the 6-s bond, such that methyl 18 alternately approaches H7 and H8 over time. For example, motion alternating between a 6-s torsion angle of ca. −70° and −120° could produce the simultaneous appearance of cross-peaks 8−18 and 7−18 of the observed intensity. This raises another difficulty. For any 6-s conformation which brings methyl 18 close enough to H7 to produce a significant NOE cross-peak, an even stronger cross-peak should appear to either methyl 16 or 17 (Figure 8). However, no such cross-peaks exist in the NOESY data set (upper portion of boxed peaks, top panel, Figure 6). It is possible that motion about the 6-s bond could account for the absence of these peaks, as the NOE cross-relaxation rate between spins can be reduced by internal motion (Olejniczak et al., 1984; Post, 1992). Motion can differentially affect each NOE interaction for a given proton as well (Post, 1992).

There is precedent for such motion. The appearance of simultaneous NOEs from methyl 18 to H7 and H8 has been observed for retinoic acid analogs freely dissolved in solution at ambient temperatures but not at −50 °C, leading to the conclusion that the β-ionone ring moves through a larger range of 6-s torsion angles at the higher temperature (Honig et al., 1971). It is thus quite possible that CRABP-I allows retinoic acid the freedom to move its ring in this fashion, while CRABP-II does not. This suggestion of motion is consistent with poor resolution of the β-ionone ring observed in the X-ray crystal structure of retinoic acid complexed with CRABP-I (Kleywegt et al., 1994). Motion of bound ligand is not without precedent for iLBPs, as motion has been detected for retinol analogs bound to CRBPII (Rong et al., 1994). In addition, the crystal structure of CRBPII shows that retinol itself adopts a 6-s torsion angle ranging from

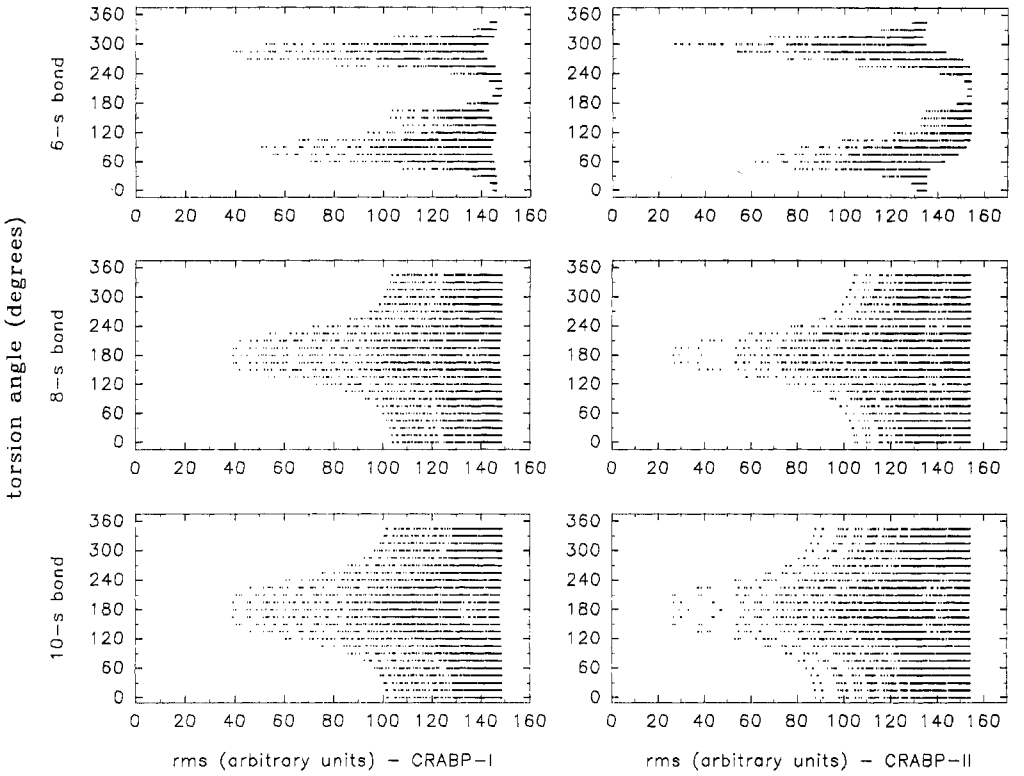

FIGURE 7: Best fit rms error values are shown for CRABP-I (left panels) and CRABP-II (right panels) bound retinoic acid. Theoretical NOESY cross-peak volumes were calculated from retinoic acid conformations generated by systematic search about the 6-s, 8-s, and 10-s bonds at 15° intervals and fit to the 16 possible olefinic (ω_1)−methyl (ω_2) cross-peak volumes shown in the boxed regions of Figure 6. The results shown used the full, rapid methyl rotational model and assigned the vicinal methyl at lower chemical shift to 16. The other three methyl models investigated yielded very similar plots. As detailed in the text, the best fit conformation for CRABP-I fails to predict the observed pattern of NOEs, probably due to motion about 6-s bond.

Table 1: Experimental versus Modeled Relative NOESY Cross-Peak Volumes for the Best Conformations[a]

	CRABP-I		CRABP-II	
proton pair	experimental	modeled	experimental	modeled
7−18	45.8 ± 10.1	14.3	0 ± 5.2	11.1
7−17	9.6 ± 13.6	21.0	16 ± 5.9	26.2
7−16	0 ± 4.9	11.5	0 ± 5.2	16.9
7−19	94.3 ± 11.2	96.4	100 ± 15.4	101.3
8−18	31.0 ± 15.7	25.3	74.5 ± 15.0	68.9
8−17	13.4 ± 6.6	1.3	1.1 ± 7.6	1.2
8−16	13.9 ± 12.2	17.2	5.5 ± 6.2	8.9
8−19	0 ± 4.9	5.9	0 ± 5.2	6.2
10−18	0 ± 4.9	1.9	0 ± 5.2	3.5
10−17	0 ± 4.9	0.2	0 ± 5.2	0.2
10−16	0 ± 4.9	1.3	0 ± 5.2	0.8
10−19	0 ± 4.9	6.8	0 ± 5.2	7.1
11−18	0 ± 4.9	0.3	0 ± 5.2	0.4
11−17	0 ± 4.9	0.1	0 ± 5.2	0.1
11−16	0 ± 4.9	0.3	0 ± 5.2	0.3
11−19	100 ± 11.4	99.0	89.6 ± 14.7	82.9

[a] Experimental NOESY cross-peaks volumes were measured in arbitrary units from the boxed portion of the isotope-filtered NOESY experiments shown in Figure 6. Modeled volumes represent the best fitting conformations using the full, rapid methyl rotational model and assigning the vicinal methyl at lower chemical shift to 16. Experimental uncertainties were estimated from the standard errors of multiple (≥3) volume measurements plus the standard error of background.

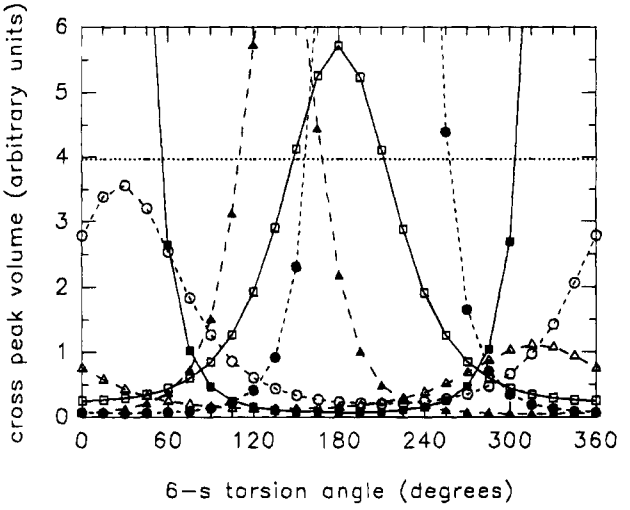

FIGURE 8: Dependence of relative NOESY cross-peak volumes on the 6-s torsion angle. Cross-peak volumes were calculated using the full, rapid methyl rotation model for CH(7)−CH_3(18) (□), CH(7)−CH_3(17) (△), CH(7)−CH_3(16) (○), CH(8)−CH_3(18) (■), CH(8)−CH_3(17) (▲), and CH(8)−CH_3(16) (●). The horizontal line represents the maximum cross-peak volume attainable for CH(7)-CH_3(19).

−78° to −150° when bound to the four distinct CRBPII molecules in the unit cell (Winter et al., 1993).

The shortest possible mixing times were employed to minimize the effects of spin diffusion. However, we cannot completely exclude that differences in intermolecular spin diffusion pathways between the two CRABPs may account for the dissimilarity in NOE patterns. Note, though, that the existence of different spin diffusion pathways would necessarily involve differences in protein−ligand interaction near the 6-s bond.

Ligand−Protein Close Contacts. A number of intermolecular NOE cross-peaks between the labeled ligand protons and protein protons can be observed in the isotope-edited NOESY spectra (see nonboxed areas of Figures 5 and 6). Proton resonance assignments have been reported for the CRABP-I/retinoic acid complex at pH 3.8 (Rizo et al.,

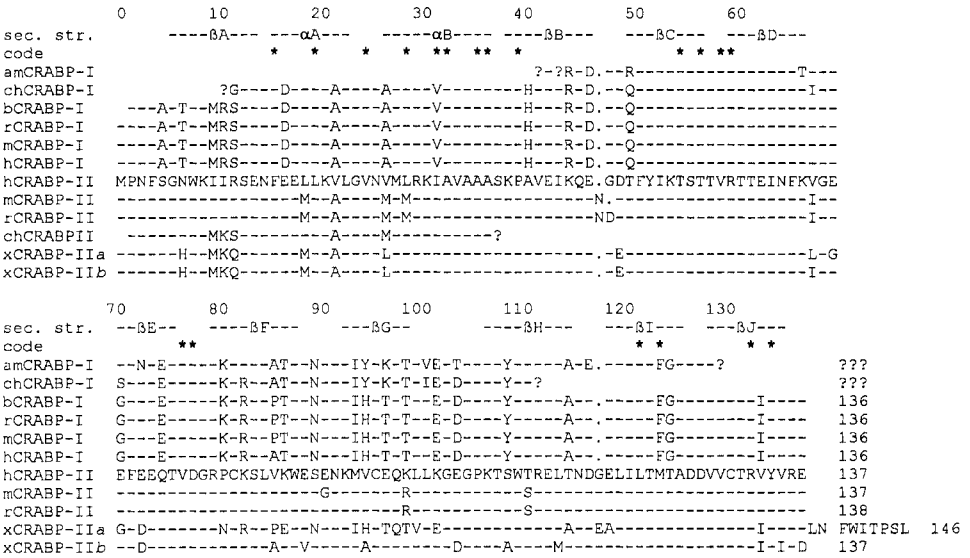

FIGURE 9: Sequence alignment of CRABP-I and CRABP-II from various organisms. Numbering is for mCRABP-II, with the initiator methionine as zero. Secondary structure is as reported (Kleywegt et al., 1994). Residues which approach bound retinoic acid within 3.5 Å, as determined from the crystal structures of CRABP-I and -II (Kleywegt et al., 1994), are marked with an asterisk (*). Abbreviations and sources: *Ambystoma mexicanum*, amCRABP-I (Ludolph et al., 1993); *Gallus gallus*, chCRABP-I (Vaessen et al., 1990), chCRABP-II (Kitmoto et al., 1989); *Bos primigenius taurus*, bCRABP-I (Crabb & Saari, 1986); *Mus sp.*, mCRABP-I (Stoner & Gudas, 1989); *Mus musculus*, mCRABP-II (MacGregor et al., 1992); *Homo sapiens*, hCRABP-I and -II (Åström et al., 1991); *Rattus norvegicus*, rCRABP-I (Rajan et al., 1991), rCRABP-II (Bucco et al., 1995); *Xenopus laevis*, xCRABP [*a*, Dekker et al. (1994); *b*, Ho et al. (1994)]. We have tentatively assigned both xCRABPs as CRABP-II's, solely on the basis of sequence comparison.

1994). Unfortunately, these assignments may not be directly applicable to our experiments, since we have observed significant differences in the "fingerprint" region of 2D proton TOCSY experiments we have performed at pH 7.4, compared to those reported at pH 3.8.

As can be seen in Figures 5 and 6, the majority of the intermolecular cross-peaks are conserved between CRABP-I and CRABP-II. Qualitative differences can be noted, however, particularly for $CH_2(3)$ and $CH_3(16,17)$. In the isotope-edited NOESY spectrum of CRABP-I/ligand **1**, an intense NOE between $CH_2(3)$ and an unlabeled proton resonance at 1.05 ppm can be observed, which is markedly less intense or missing for CRABP-II/ligand **1**. Instead, a cross-peak between $CH_2(3)$ and a proton resonance at 1.99 ppm is observed in the isotope-edited NOESY spectrum of CRABP-II/ligand **1**, but not of CRABP-I/ligand **1** (see starred peaks of Figure 5). Prominent NOESY cross-peaks between $CH_3(16,17)$ and proton resonances at 2.10 and 2.01 ppm were observed only for the CRABP-II/ligand **2** complex, and not for the CRABP-I/ligand **2** complex (see starred peaks of Figure 6), suggesting a ligand−protein close contact at this position for CRABP-II but not CRABP-I. Unambiguous identification of the protein residues involved in these interactions awaits total assignment of holo-CRABP-I at pH 7.4 or site-directed mutagenesis experiments.

DISCUSSION

The crystal structures for mouse CRABP-I and human CRABP-II complexed with *all-trans*-retinoic acid have been recently reported, at resolutions of 2.9 and 1.8 Å, respectively (Kleywegt et al., 1994). The resolution of the CRABP-II electron densities allowed the vicinal methyls 16 and 17 to be distinguished from methyl 18. This allowed determination of the torsion angle between the β-ionone ring and the polyene chain at −33°. Because of inability to fit the β-ionone ring to the CRABP-I X-ray data, retinoic acid was directly copied from the final CRABP-II X-ray structure and fitted to the CRABP-I electron densities as a rigid body. Hence, conclusions regarding the 6-s torsion angle for CRABP-I bound retinoic acid are limited. The NMR determined torsion angle for CRABP-II is in agreement with the X-ray study. Both methods show a distorted 6-s *cis* conformation for bound retinoic acid as well as *trans* configurations for 8-s and 10-s. The NMR measurements suggest a slightly larger 6-s skew of ca. −60° compared to the crystal data. This may reflect differences between mouse and human CRABP-II, differences between the crystalline and solution states, or uncertainties in either technique. Alternatively, modest rotation of the 8-s bond from a *trans* configuration (i.e., 180°± 30°) could reduce the skew introduced by the −60° 6-s torsion angle, bringing the overall ring/chain angle closer to −33°.

The differences observed in intermolecular cross-peaks between CRABP-I and CRABP-II are consistent with amino acid substitution between the two proteins (Figure 9), as shown by examination of the X-ray structures. We have tentatively identified the NOESY cross-peak partner of CH_2-(3) (ω_2) at 1.05 ppm (ω_1) to be H^δ of Leu 28, for the CRABP-I−ligand **1** complex. The amino acid at position 28 in mouse CRABP-II is a methionine, accounting for the absence of a cross-peak at this position and the appearance of a new cross-peak for $CH_2(3)$ (ω_2) at 1.99 ppm (ω_1), possibly corresponding to H^γ or H^ε of Met 28. In the X-ray structures, $CH_2(3)$ closely approaches (<2.5 Å) Leu/Met 28. Note that the amino acid substitution at residue 28 is not conserved to other species. The cross-peaks for $CH_3(16,$-17) (ω_2) at 2.1 ppm (ω_1), found in CRABP-II only, are potentially consistent with H^β of Ile 31, which approaches $CH_3(16,17)$ within 3 Å in the CRABP-II crystal structure. In CRABP-I, position 31 is a valine and may not interact with $CH_3(16,17)$ in the same manner. This substitution at residue 31 is highly conserved (Figure 9). The only other substitution near bound retinoic acid is F122 in CRABP-I to M123 in CRABP-II. However, this residue is located near

the carboxylic end of retinoic acid, which we could not observe using our ^{13}C-labeled compounds.

The presented isotope-edited NMR experiments have suggested differences in the conformation and motion of retinoic acid when bound to CRABP-I and CRABP-II. These experiments have also determined differences in the atoms neighboring retinoic acid which can be ascribed to amino acid substitution between CRABP-I and CRABP-II. The significance of these findings with respect to binding specificity will be tested further by modifying the ligand–protein interface at these positions by site-directed mutagenesis of the protein and synthetic modification of retinoic acid.

ACKNOWLEDGMENT

Cindy Jenkins kindly expressed and purified the protein used in these studies. We thank Denise Beusen, David Cistola, Jay Ponder, and Michael Hodsdon for insightful discussions and assistance. We thank Alwyn Jones for providing us with the crystal structure coordinates of holo CRABP-I and CRABP-II.

SUPPORTING INFORMATION AVAILABLE

Two tables listing resonance assignments and best fitting conformations (2 pages). Ordering information is given on any current masthead page.

REFERENCES

Åström, A., Tavakkol, A., Pettersson, U., Cromie, M., Elder, J. T., & Voorhees, J. J. (1991) *J. Biol. Chem. 266*, 17662.
Bailey, J. S., & Siu, C.-H. (1988) *J. Biol. Chem. 263*, 9326.
Banaszak, L., Winter, N., Xu, Z., Bernlohr, D. A., Cowan, S., & Jones, T. A. (1994) *Adv. Protein Chem. 45*, 89.
Bax, A., & Davis, D. G. (1985) *J. Magn. Reson. 65*, 355.
Becker, R. S., Berger, S., Dalling, D. K., Grant, D. M., & Pugmire, R. J. (1974) *J. Am. Chem. Soc. 96*, 7008.
Boylan, J. F., & Gudas, L. J. (1991) *J. Cell. Biol. 112*, 965.
Bucco, R. A., Melner, M. H., Gordon, D. S., Leers-Sucheta, S., & Ong, D. E. (1995) *Endocrinology 136*, 2730.
Crabb, J. W., & Saari, J. C. (1986) *Biochem. Int. 12*, 391.
Dekker, E.-J., Vaessen, M.-J., van den Berg, C., Timmermans, A., Godsave, S., Holling, T., Nieuwkoop, P., Geurts van Kessel, A., & Durston, A. (1994) *Development 120*, 973.
Fesik, S. W. (1993) *J. Biomol. NMR 3*, 261.
Fesik, S. W., Eaton, H. L., Olejniczak, E. T., & Zuiderweg, E. R. P. (1990a) *J. Am. Chem. Soc. 112*, 886.
Fesik, S. W., Gampe, R. T., Jr., Holzman, T. F., Egan, D. A., Edalji, R., Luly, J. R., Simmer, R., Helfrich, R., Kishore, V., & Rich, D. H. (1990b) *Science 250*, 1406.
Fiorella, P. D., & Napoli, J. L. (1991) *J. Biol. Chem. 266*, 16572.
Fiorella, P. D., Giguère, V., & Napoli, J. L. (1993) *J. Biol. Chem. 268*, 21545.
Giguère, V., Lyn, S., Yip, P., Siu, C.-H., & Amin, S. (1990) *Proc. Natl. Acad. Sci. U.S.A. 87*, 6233.
Gronenborn, A. M., Bax, A., Wingfield, P. T., & Clore, G. M. (1989) *FEBS Lett. 243*, 93.
Harbison, G. S., Smith, S. O., Pardoen, J. A., Courtin, J. M. L., Lugtenburg, J., Herzfeld, J., Mathies, R. A., & Griffin, R. G. (1985) *Biochemistry 24*, 6955.
Ho, L., Mercola, M., & Gudas, L. J. (1994) *Mech. Dev. 47*, 53.
Hong, W. K., & Itri, L. M. (1994) in *The Retinoids: Biology, Chemistry, and Medicine* (Sporn, M. B., Roberts, A. B., & Goodman, D. S., Eds.) pp 597–630, Raven Press, New York.
Honig, B., Hudson, B., Sykes, B. D., & Karplus, M. (1971) *Proc. Natl. Acad. Sci. U.S.A. 68*, 1289.
Kaegi, H. H., & DeGraw, J. I. (1981) *J. Labelled Comp. Radiopharm. XVIII*, 1099.
Kitamoto, T., Momoi, T., & Momoi, M. (1989) *Biochem. Biophys. Res. Commun. 159*, 371.
Kleywegt, G. J., Bergfors, T., Senn, H., Le Motte, P., Gsell, B., Shudo, K., & Jones, T. A. (1994) *Structure 2*, 1241.
Ludolph, D. C., Cameron, J. A., Neff, A. W., & Stocum, D. L. (1993) *Dev. Growth Differ. 35*, 341.
MacGregor, T. M., Copeland, N. G., Jenkins, N. A., & Giguère, V. (1992) *J. Biol. Chem. 267*, 7777.
Mangelsdorf, D. J., Umesono, K., & Evans, R. M. (1994) in *The Retinoids: Biology, Chemistry, and Medicine* (Sporn, M. B., Roberts, A. B., & Goodman, D. S., Eds.) pp 319–350, Raven Press, New York.
Marion, D., & Wüthrich, K. (1983) *Biochem. Biophys. Res. Commun. 113*, 967.
Morikis, D., Brüschweiler, R., & Wright, P. E. (1993) *J. Am. Chem. Soc. 115*, 6238.
Norris, A. W., Cheng, L., Giguère, V., Rosenberger, M., & Li, E. (1994) *Biochim. Biophys. Acta 1209*, 10.
Olejniczak, E. T., Dobson, C. M., Karplus, M., & Levy, R. M. (1984) *J. Am. Chem. Soc. 106*, 1923.
Ong, D. E., & Chytil, F. (1978) *J. Biol. Chem. 253*, 4551.
Peck, G. L., DiGiovanna, J. J. (1994) in *The Retinoids: Biology, Chemistry, and Medicine* (Sporn, M. B., Roberts, A. B., & Goodman, D. S., Eds.) pp 631–658, Raven Press, New York.
Pegg, D. T., Bendall, M. R., & Doddrell, D. M. (1980) *Aust. J. Chem. 33*, 1167.
Petkovich, M. (1992) *Annu. Rev. Nutr. 12*, 443.
Post, C. B. (1992) *J. Mol. Biol. 224*, 1087.
Rajan, N., Kidd, G. L., Talmage, D. A., Blaner, W. S., Suhara, A., Goodman, D. S. (1991) *J. Lipid Res. 32*, 1195.
Rizo, J., Liu, Z.-P., & Gierasch, L. M. (1994) *J. Biomol. NMR 4*, 741.
Rong, D., Lovey, A. J., Rosenberger, M., d'Avignon, D. A., & Li, E. (1994) *Biochim. Biophys. Acta 1208*, 136.
Rowan, R., III, & Sykes, B. D. (1974) *J. Am. Chem. Soc. 96*, 7000.
Rowan, R., III, Warshel, A., Sykes, B. D., & Karplus, M. (1974) *Biochemistry 13*, 970.
Ruberte, E., Friederich, V., Morriss-Kay, G., & Chambon, P. (1992) *Development 115*, 973.
Scott, W. J., Jr., Walter, R., Tzimas, G., Sass, J. O., Nau, H., & Collins, M. D. (1994) *Dev. Biol. 165*, 397.
Shaka, A. J., Barker, P. B., & Freeman, R. (1985) *J. Magn. Reson. 64*, 547.
Siegenthaler, G., Tomatis, I., Chatellard-Gruaz, D., Jaconi, S., Eriksson, U., & Saurat, J.-H. (1992) *Biochem. J. 287*, 383.
Stam, C. H. (1972) *Acta Crystallogr. B28*, 2936.
Stam, C. H., & MacGillavry, C. H. (1963) *Acta Crystallogr. 16*, 62.
States, D. J., Haberkorn, R. A., & Ruben, D. J. (1982) *J. Magn. Reson. 48*, 286.
Stoner, C. M., & Gudas, L. J. (1989) *Cancer Res. 49*, 1497.
Summers, M. F., Marzilli, L. G., & Bax, A. (1986) *J. Am. Chem. Soc. 108*, 4285.
Vaessen, M.-J., Meijers, J. H. C., Bootsma, D., & Geurts van Kessel, A. (1990) *Development 110*, 371.
Waterhous, D. V., & Muccio, D. D. (1990) *Magn. Reson. Chem. 28*, 223.
Wider, G., Weber, C., Traber, R., Widmer, H., & Wüthrich, K. (1990) *J. Am. Chem. Soc. 112*, 9015.
Winter, N. S., Bratt, J. M, & Banaszak, L. J. (1993) *J. Mol. Biol. 230*, 1247.

BI951340D